# Molecular mechanisms underlying mifepristone's agonistic action on ovarian cancer progression

Donata Ponikwicka-Tyszko [a], Marcin Chrusciel [b], Joanna Stelmaszewska [c], Piotr Bernaczyk [d], Paulina Chrusciel [e], Maria Sztachelska [a], Mika Scheinin [f], Mariusz Bidzinski [g], Jacek Szamatowicz [h], Ilpo T. Huhtaniemi [b,i], Slawomir Wolczynski [a,c], Nafis A. Rahman [b,c,*]

[a] Department of Biology and Pathology of Human Reproduction, Institute of Animal Reproduction and Food Research, Polish Academy of Sciences, Olsztyn, Poland
[b] Institute of Biomedicine, University of Turku, Finland
[c] Department of Reproduction and Gynecological Endocrinology, Medical University of Bialystok, Poland
[d] Department of Medical Pathomorphology, Medical University of Bialystok, Poland
[e] Central Animal Laboratory, University of Turku, Turku, Finland
[f] Department of Pharmacology, Drug Development and Therapeutics, University of Turku, Turku, Finland
[g] Department of Gynecological Oncology, Maria Sklodowska - Curie Institute Oncology Center, Warsaw, Poland
[h] Department of Gynecology and Gynecological Oncology, Medical University of Bialystok, Poland
[i] Institute of Reproductive and Developmental Biology (IRDB), Imperial College London, London, UK

## ARTICLE INFO

## ABSTRACT

Background: Recent clinical trials on ovarian cancer with mifepristone (MF) have failed, despite in vitro findings on its strong progesterone (P4) antagonist function.
Methods: Ovarian cancer human and murine cell lines, cultured high-grade human primary epithelial ovarian cancer (HG-hOEC) cells and their explants; as well as in vivo transgenic mice possessing ovarian cancer were used to assess the molecular mechanism underlying mifepristone (MF) agonistic actions in ovarian cancer progression.
Findings: Herein, we show that ovarian cancer cells express traceable/no nuclear P4 receptor (PGR), but abundantly P4 receptor membrane component 1 (PGRMC1). MF significantly stimulated ovarian cancer cell migration, proliferation and growth in vivo, and the translocation of PGRMC1 into the nucleus of cancer cells; the effects inhibited by PGRMC1 inhibitor. The beneficial antitumor effect of high-doses MF could not be achieved in human cancer tissue, and the low tissue concentrations achieved with the therapeutic doses only promoted the growth of ovarian cancers.
Interpretation: Our results indicate that treatment of ovarian cancer with MF and P4 may induce similar adverse agonistic effects in the absence of classical nuclear PGRs in ovarian cancer. The blockage of PGRMC1 activity may provide a novel treatment strategy for ovarian cancer.
Fund: This work was supported by grants from the National Science Centre, Poland (2013/09/N/NZ5/01831 to DP-T; 2012/05/B/NZ5/01867 to MC), Academy of Finland (254366 to NAR), Moikoinen Cancer Research Foundation (to NAR) and EU PARP Cluster grant (UDA-POIG.05.01.00-005/12-00/NCREMFP to SW).

**Research in context**

*Evidence before this study*

Selective progesterone receptor modulator mifepristone (MF) has been and still is with several ongoing clinical trials an attractive therapeutic target in many cancers. However, all clinical trials targeting progesterone receptors (PRGs) with MF have largely been unsuccessful without showing reasons.

*Added value of this study*

In this study, we tried to reveal the molecular mechanism underlying mifepristone (MF) agonistic actions in ovarian cancer progression using ovarian cancer human and murine cell lines, cultured high-grade human primary epithelial ovarian cancer (HG-hOEC) cells and their explants; as well as *in vivo* transgenic mice possessing ovarian cancer. We showed that MFs failure in anti-cancer therapy is due to its agonistic membrane progesterone receptor (PGRMC1) action that enhances tumor growth.

*Implications of all the available evidence*

Mifepristone (MF) appears ineffective in anti-cancer therapy due to its agonistic membrane progesterone receptor (PGRMC1) providing the mechanism of tumor growth enhancing activity. PGRMC1 inhibitors can provide an important therapeutic means for the treatment of high-grade human epithelial ovarian cancer.

# 1. Introduction

Mifepristone (MF, RU486, a selective progesterone receptor modulator (SPRMs) with a strong antagonist activity to the nuclear progesterone receptor (PGR) is receiving increasing attention as a potential anti-cancer agent due to its antiprogestin activity and numerous cancers steroid-dependency and PGR expression [1–6]. MF may also act as a PGR agonist, as shown in human mammary gland carcinoma cells, through interactions with different PGR isoforms [7,8]. Progesterone (P4) signal may also be transduced through rapid non-genomic events *via* membrane P4 receptors (mPR) α, β and γ; PGRMC1; and PGRMC2 [9]. However, the type of PR that can serve as the potential mediator(s) of P4 and MF actions in ovarian cancers remains unknown [10–13].

MF inhibits ovarian, breast, nervous system, prostate, ovarian, and bone cancer cell growth *in vitro* in a time- and dose-dependent manner [10–14]. MF clinical trials of several cancers (human refractory and re-current/persistent ovarian, fallopian tube, primary peritoneal, recurrent endometrioid adenocarcinomas or low-grade (LG) endometrial stromal sarcomas, meningiomas and breast cancers) were unsuccessful [1–6]. A phase-2 MF clinical trial (200 mg/day) for the treatment of recurrent, cisplatin- and paclitaxel-resistant ovarian epithelial cancer resulted in partial positive responses in 26.5% of women [1]. The results of another phase 2 trial with advanced ovarian, peritoneal and fallopian tube cancers were more disappointing [2], with 1/22 with partial remission, 15/22 showing cancer progression [2]. In a third study with PGR-positive advanced or recurrent endometrioid adenocarcinoma or LG endometrial stromal sarcoma, an 8-week (200 mg/day) MF treatment was associated with cancer progression in 75% of the patients, with no partial or complete responses [3]. Moreover, in metastatic breast cancers, treatment with MF (200 or 400 mg/day) resulted in partial positive responses in only 1/11, and in 36% patients marked disease progression [15]. Other possible mediators of MF actions in cancers are the glucocorticoid receptors (GRs) as MF is also a glucocorticoid antagonist [7,12].

However, in ovarian cancer cells, MF did not affect the levels of $GR\alpha$ or $GR\beta$ expression and did not activate GRs in high-grade (HG) serous ovarian carcinomas [12,16]. The explanation of the MF treatment failure has become even more important because further clinical trials (at least 7) on MF are being carried out (ClinicalTrials.gov identifier: NCT02046421, NCT02651844, NCT01898312, NCT02014337, NCT01493310, NCT02012296 and NCT02642939).

The reasons behind the clinical trials failure, as well as the discrepancy between the outcomes of MF effects *in vivo* and *in vitro,* remain unclear. Due to the lack of an appropriate experimental mouse model for human epithelial ovarian cancer [17], we used transgenic (TG) mice expressing Simian Virus 40 T antigen under the inhibin α promoter (Inhα/Tag) that develops granulosa cell tumors (GCTs) by 5 months of age with 100% penetrance, and metastasize to the lung and liver (10%) [18,19]. For *in vitro* experiments, we used immortalized murine KK-1 cells from Inhα/Tag TG mice and high-grade human primary epithelial ovarian cancer (HG-hOEC) cells, and their explants. Our aim was to study the antagonistic/agonistic role of MF and its influence on the mechanisms involved in ovarian cancer progression. We also monitored the pharmacokinetics of MF and its metabolites at clinically relevant doses to analyze whether they were sufficient.

# 2. Materials and methods

## 2.1. Experimental animals

*In vivo* studies were done on transgenic mice expressing Simian Virus 40 T antigen under the Inhibin α promoter (Inhα/Tag) TG mice, previously characterized [18–19]. The 5.5 months of age female mice with discernible ovarian tumors were randomized into three groups ($n = 10$ mice/group) and intraperitoneally injected every 2 days with vehicle (corn oil), MF (10 mg/kg) or P4 (1 mg/kg) for 1 month. Treatment of the ovarian tumors started at the age 5.5 months in order to ensure appearance of advanced tumorigenesis. The mice were fed with mouse chow SDS RM-3 (Special Diet Service; E, soy free; Whitham Essex, UK), tap water *ad libitum* and kept in a specific pathogen-free surrounding and routinely screened for common mouse pathogens. After 30 days of treatments mice were sacrificed, blood samples were collected and tumors were excised and weighed. Half of each tumor was fixed in 4% paraformaldehyde and embedded in paraffin for histological and immunohistochemical studies. The second half of the tumor tissue was snap-frozen in liquid nitrogen and stored at −80 °C for RT-PCR analysis.

## 2.2. Human tissue samples

Fresh tissue samples from hEOC patients ($n = 60$) were collected immediately after surgery at Department of Gynecology and Gynecological Oncology, Medical University of Bialystok, Poland and Department of Gynecological Oncology, Maria Sklodowska - Curie Institute Oncology Center, Warsaw, Poland for the *in vitro* studies. All the samples were histologically examined at Department of Medical Pathomorphology, Medical University of Bialystok, Poland in order to prove the tumor grade. Archival human ovarian tumors paraffin blocks ($n = 90$) for immunohistochemistry analyses were obtained from the Department of Medical Pathomorphology; Medical University of Bialystok, Bialystok, Poland.

### 2.2.1. Ethics approval and consent to participate

The Ethics Committee for animal experimentation of the University of Turku and the State Provincial Office of Southern Finland approved all animal experiments. The Human Investigation Ethics Committees in Bialystok (Medical University of Bialystok) and Warsaw (Maria Sklodowska - Curie Institute Oncology Center, Warsaw, Poland) approved the study. Written informed consent was obtained at the time of the surgery from all patients' prior inclusion.

## 2.3. Drugs and inhibitors

Mifepristone (MF), progesterone (P4) and PGRMC1 inhibitor (AG-205) were provided by Sigma-Aldrich (Saint Louis, MO, USA). 22-hydroxy (H948445), Di-demethyl (D439550) and N-demethyl mifepristone (D230950) were ordered from Toronto Research Chemicals Inc. (Toronto, Ontario, Canada). TGFBRI/RII inhibitor (GW788388) and HSP90 inhibitor (Geldanamycin) was purchased from Selleck Chemicals (Houston, TX, USA).

## 2.4. Cell cultures

### 2.4.1. Murine cell line culture and stimulation

The murine granulosa tumor cell line (KK−1) [18] was cultured in DMEM/F12 medium (GIBCO, Paisley, UK) supplemented with 10% fetal bovine serum (FBS; Biochrom, Berlin, Germany), 100 units/ml penicillin and 100 μg/ml streptomycin (P/S solution; Sigma-Aldrich) at 37 °C in a humidified atmosphere in the presence of 5% CO2. For final cell proliferation analyses, $8 \times 10^3$ KK-1 cells/well were seeded onto 96-well plate and treated with vehicle (0), MF (0.01; 1; 2; 3; 5; 7; 17; 25 μM), P4 (0.0003; 0.003; 0.03; 0.3; 3 μM), 22-hydroxy, Di-demethyl and N-demethyl MF (1; 2; 5; 17 μM), 10 μM TGFβ1 (240-B; R&D Systems Inc., Minneapolis, MN), TGFβ1 (10 μM) + MF (5 μM), TGFβ1 (10 μM) + P4 (0.3 μM), AG-205 (1 μM), AG-205 (1 μM) + MF (5 μM) or AG-205 (1 μM) + P4 (0.3 μM) in stimulation medium [phenol-free DMEM/F12 with 0.5% charcoal-stripped FBS and P/S solution]. For hormone measurements and gene expression analyses $3.5 \times 10^5$ onto 6-well plate/well and treated with vehicle (0), TGFβ1 (10 μM), MF (5 μM) or P4 (0.3 μM) in stimulation medium. Three independent experiments in octuplicate (96-well plate) or triplicate (6-well plate) were performed for each treatment.

### 2.4.2. Primary hEOC culture and stimulation

Fresh HG hEOC tissues samples ($n = 10$) were washed twice with PBS, cut into small pieces and digested enzymatically with collagenase type II (Sigma). After digestion, cells were maintained in RPMI-1640/Ham's F12 (GIBCO) media supplemented with 10% fetal bovine serum and P/S solution at 37 °C in a humidified atmosphere in the presence of 5% CO2. For final cell proliferation analyses, $9 \times 10^3$ HG hEOC cells/well were seeded onto 96-well plate and treated with vehicle (0), MF (0.01; 1; 2; 3; 5; 7; 17; 25 μM), P4 (0.0003; 0.003; 0.03; 0.3; 3 μM), AG-205 (1 μM), AG-205 (1 μM) + MF (3 μM), AG-205 (1 μM) + P4 (0.3 μM), TGFβ1 (10 μM), TGFβ1 (10 μM) + MF (3 μM) or TGFβ1 (10 μM) + P4 (0.3 μM) in stimulation medium [phenol-free RPMI-1640/Ham's F12 1:1 with 0.5% charcoal-stripped FBS and P/S solution]. Three independent experiments in octuplicate were performed for each treatment.

### 2.4.3. hOEC explants culture and stimulation

Fresh HG hEOC tissues samples ($n = 10$) were washed twice with PBS and cut into ~1-mm diameter pieces on a petri dish with a sterile scalpel. Explants were plated onto 24-well plates and maintained in RPMI-1640/Ham's F12 1:1 media supplemented with 10% fetal bovine serum and P/S solution at 37 °C in a humidified atmosphere in the presence of 5% CO2. After 2-days the explants were treated with either vehicle (0), MF (3 μM), P4 (0.03; 0.3; 3 μM), AG-205 (1 μM), AG-205 (1 μM) + MF (3 μM) and AG-205 (1 μM) + P4 (0.3 μM) in stimulation medium for an additional 24 h. Next, culture medium was collected for hormone measurements and explants for RNA extraction and gene expression analyses. Three independent experiments in quadruplicates were performed for each treatment.

## 2.5. Cell proliferation

Cell proliferation was evaluated in KK-1 and primary HG hOEC cell line using CellTiter 96® AQueous Non-Radioactive Cell Proliferation Assay (Promega, Madison, Wisconsin, USA) and BrdU Cell Proliferation Assay Kit (Cell Signaling Technology, Danvers, MA) after 72 h of treatments. Medium containing fresh doses of drugs was changed every 24 h. Control groups were treated with vehicle ethanol at a final concentration of 0.05% of ethanol. In BrdU assay cells were exposed to 10 μM 5-bromo-2′-deoxyuridine (BrdU) for 12 h. Next, cells were fixed and anti-BrdU antibody was added. Incorporation of BrdU into the DNA was assessed through absorbance magnitude measurements. The proliferation of the treated groups was presented as percentage of control proliferation considered as 100%. Three independent experiments per cell line were run, each performed in octuplicate wells.

## 2.6. Cell invasion

Cell invasion intensity of KK-1 and primary HG hOEC cell lines was assessed using CultreCoat® Cell Invasion Assays (R&D Systems). Briefly, $2.5 \times 10^4$ cells/well were transferred to each of 96-well plate top invasion chamber coated with Basement Membrane Extract (BME). Cells invaded in response to steroids (MF and P4) and AG-205 (1 μM) were quantitated using Calcein AM after 24 h of treatment. Three independent experiments per cell line were run, each performed in octuplicate wells. Cell invasion intensity of the treated groups was presented as percentage of invasion of control group, considered as 100%.

## 2.7. Pharmacokinetics analyses

For pharmacokinetic analyses, 6 mo-old females Inhα/Tag TG mice with discernible tumors were intraperitoneally injected with a single dose of 1 mg/kg of MF ($n = 10$) and 10 mg/kg of MF ($n = 10$). Blood samples were collected at several time points: after 30 min, 4 h, and 8 h, 16 h, 24 h and 48 h. Then, concentrations of MF and its metabolites N-demethyl MF, Di-demethyl MF and 22-hydroxyl MF in mouse plasma were determined using high performance liquid chromatography–mass spectrometry (HPLC-MS/MS) after protein precipitation with internal standard alfaxalone. HPLC separation was performed with Agilent 1200 LC system, using a C18 column. Multiple-reaction monitoring with a triple quadrupole mass spectrometer was used for quantitative analyses (AB Sciex 4000 QTrap with Analyst software (v. 1.6.1); MDS Sciex, Ontario, Canada).

## 2.8. Real time RT-PCR

Total RNA from cells, explants and snap-frozen ovarian tumors were prepared using TRIzol extraction method (Invitrogen, Carlsbad, CA). The quantity and quality of isolated RNA was determined by NanoDrop (Thermo Fisher Scientific Inc., Waltham, MA, USA) and gel electrophoresis. Before the reverse transcription (RT) reaction 1 μg of total RNA was incubated for 30 min with DNase I (Invitrogen, Carlsbad, CA) at room temperature. The RT reaction was performed with DyNAmo ™ cDNA Synthesis Kit (Finnzymes, Espo. Finland) at 37 °C for 1 h in 20 μl. Quantification of investigated genes was performed with FX96™ Real-Time PCR Detection System, Bio Rad using DyNAmo SYBR Green qPCR kit (Finnzymes). Reaction conditions were: initial denaturation at 95 °C for 10 min followed by 40 amplification cycles at 95 °C for 15 s, 56–60 °C at 45 s and 70 °C at 45 s. At the end of the PCR reaction, melting curve was determined to ensure single product amplification. Amplification products were separated on 1.8% agarose gel and stained with ethidium bromide. Expression levels were normalized to the housekeeping gene peptidylprolyl isomerase (PPIA). The primer sequences and expected product sizes are shown in Supplementary Table S1.

## 2.9. Hormone and TGFβ1 measurements

Serum levels of LH and FSH were measured by immunofluorometric assays (Delfia; Perkin-Elmer-Wallac, Turku, Finland) as described
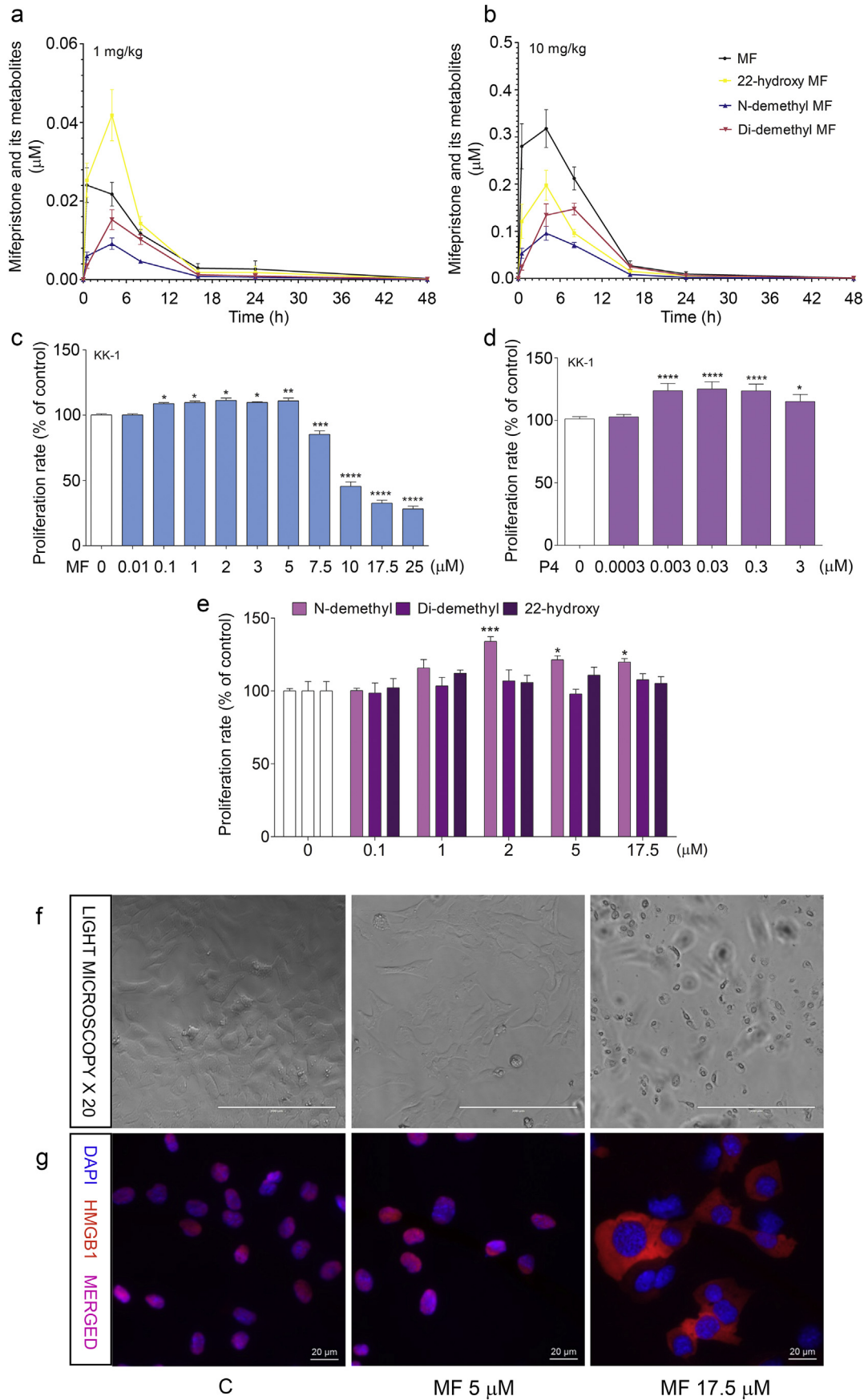
previously [20,21]. Serum P4 level was measured using Delfia Progesterone Kit (Wallac). The intra- and interassay coefficients of variations for these assays were below 10%. Serum level of inhibin B was evaluated by immunoassay Inhibin-B EIA Kit (Sigma). TGFβ1 level in serum and cell culture supernates was assessed using TGF-beta1 Quantikine ELISA Kit (R&D Systems), following the instructions of the manufacturer.

### 2.10. Histological and immunohistochemical analyses

Mouse and human ovarian tumor tissues were paraformaldehyde-fixed and embedded in paraffin. For histological analysis paraformaldehyde fixed 5 μm paraffin sections were stained with hematoxylin-eosin. For immunohistochemistry sections were deparaffinized, hydrated and boiled in 10 mM citric acid buffer (pH 6.0) in retriever for 2.5 h. Tissue sections were incubated with blocking solutions (10% normal goat serum (NGS) with 3% bovine serum albumin (BSA) or only 3% BSA in PBS) for 1 h at room temperature in order to reduce non-specific background staining. Then, sections were incubated overnight at 4 °C with the primary antibodies for PGR (MA5–12658, Thermo Fisher; dilution 1:700), mPRα (ab75508, Abcam, Cambridge, UK; dilution 1:500), mPRβ (ab46534, Abcam; dilution 1:1000), mPRγ (ab79517, Abcam; dilution 1:500), PGRMC1 (PAB20135, Abnova Corporation, Taipei, Taiwan; dilution 1:2000), PGRMC2 (ab125122, Abcam; dilution 1:1000), TGFβRII (sc-220, Santa Cruz Biotechnology, Dallas, USA; dilution) Ki-67 (Clone TEC-3, Dako, Glostrup, Denmark; dilution 1:500), SV40 Tag (DP02-200UG, Oncogene Research Products, San Diego, CA, USA; dilution 1:300). After endogenous peroxidase blocking (0.5% $H_2O_2$ in PBS for 20 min in dark at room temperature) primary antibodies were linked with Envision® anti-mouse or anti-rabbit polymer + HRP (Dako) for 30 min at room temperature, only for Ki-67 staining before this step, secondary antibody rabbit anti rat was added (Dako, dilution 1:200). The reaction product was visualized using 3′3-diaminobenzidine tetrahydrochloride (DAB, Dako). Three washes were done after each step with PBS with 0.05% Tween (PBS-T). Hematoxylin was used as counterstain and then sections were dehydrated and mounted with Pertex (Histolab Products AB).

### 2.11. Immunocytochemistry analysis

KK-1 or HG hOEC $6 × 10^3$ cells/well were seeded onto microscope slide coverslips and treated with vehicle (0), MF (5 μM), P4 (0.3 μM), vehicle (0), MF (3 μM), DXM (200 nM), MF (3 μM) + HSP90i (50 nM), HSP90i (50 nM) + DXM (200 nM) or vehicle (0), MF (3 μM), P4 (0.3 μM), AG-205 (1 μM), MF (3 μM) + AG-205 (1 μM), P4 (0.3 μM) + AG-205 (1 μM) in stimulation medium. KK-1 or HG hOEC cells were fixed in 3–4% PFA in PBS pH 7.4 for 15 min at room temperature and permeabilized for 20 min in 0.1% Triton X-100. To reduce autofluorescence cells were incubated with 100 mM NH4CL for 10 min. To block unspecific binding cells were incubated in blocking solution (3% BSA in PBS with 0.05% Tween 20) for 30 min. Next, cells were incubated for 1 h with primary antibodies GR (SC-56851, Santa Cruz Biotechnology; dilution 1:400), PGRMC1 (PAB20135, Abnova Corporation; dilution 1:1000) or HMGB1 (ab79823, Abcam; dilution 1:350) diluted in blocking solution. Next, cells were incubated with secondary fluorescent antibody Alexa Fluor 488 goat anti-mouse IgG (ab150113, Abcam; dilution 1:400) or Alexa Fluor 647 donkey anti-rabbit IgG (Life Technologies,

dilution 1:600) for 45 min. To detect cell nuclei cells were incubated with DAPI for 1 min.

### 2.12. Statistics

We used GraphPad PRISM v.6.0 (GraphPad Software, Inc., San Diego, CA) for statistical analysis by One-way ANOVA with the post-hoc Bonferroni's test. Results were expressed as mean ± SEM. The differences were considered to be significant at $p < .05$.

## 3. Results

### 3.1. MF achieves low μM serum concentrations after the administration of 10 mg/kg of MF in a pharmacokinetics study

Human pharmacological studies on MF have shown that MF and its metabolites (N-demethyl, Di-demethyl and 22-hydroxy MF) achieve low μM serum concentrations [22–26]. We evaluated their levels in the sera of Inhα/Tag TG mice. The pharmacokinetics of MF were analyzed after a single-dose i.p. injection of 1 mg/kg or 10 mg/kg MF, which corresponded to the doses used in clinical trials. MF was metabolized in a dose-dependent manner by hydroxylation and demethylation. Following injection of 1 mg/kg MF, the peak concentration of MF (0.02–0.04 μM) was evident by 0.5 h (Fig. 1a). After injection of 10-mg/kg, the peak MF concentration of 0.18 to 0.4 μM was observed at 4 h (Fig. 1b).

The peak N-demethyl MF concentrations at 4 h varied from 0.003 to 0.013 μM and 0.04 to 0.15 μM after the 1-mg/kg and 10-mg/kg injections, respectively. The peak concentrations of 22-hydroxy MF were observed at 4 h after the injections of 1 mg/kg and 10 mg/kg MF at 0.014–0.037 and 0.084–0.28 μM, respectively. The serum levels of 22-hydroxy MF at 0.5 h after a single injection of 1 mg/kg MF were similar to the serum levels of MF and exceeded those of MF at 4 h (Fig. 1a). The highest serum concentrations (0.09–0.18 μM) of Di-demethyl MF after 10 mg/kg MF were observed at 8 h.

### 3.2. MF and P4 stimulate ovarian cancer cell proliferation in vitro

As the pharmacokinetic studies confirmed that in mouse serum, MF achieved low μM concentrations, we analyzed the effects of 0.01–25 μM MF and 0.1–17.5 μM MF metabolites, which encompassed the MF doses used previously, on KK-1 cell proliferation [10–14]. We also verified the effects of 0.003, 0.03, 0.3 and 3 μM P4 as a comparative group to distinguish between the antagonistic/agonistic effects of MF. Clinically relevant doses of MF, up to 5 μM (Fig. 1c), and of P4 (0.003, 0.03, 0.3 and 3 μM) (Fig. 1d) significantly stimulated the proliferation of KK-1 cells compared to non-stimulated controls. Higher doses of MF (from 7.5 to 25 μM) significantly inhibited cell proliferation (Fig. 1c). Similarly, treatment with N-demethyl MF significantly stimulated cell proliferation (Fig. 1e). The other MF metabolites (Di-demethyl and 22-hydroxy MF) did not affect cancer cell proliferation (Fig. 1e).

Additionally, to investigate whether the lower doses of MF induced cell death, we analyzed the translocation of HMGB1 protein as a marker of cell death. We observed HMGB1 translocation from the nucleus to the cytoplasm in KK-1 cells with 17.5 μM MF but not with 5 μM MF (Fig. 1g).

---

**Fig. 1.** Metabolism of MF in Inhα/Tag TG mice and proliferation of KK-1 cells with MF, P4 or MF metabolite treatment. Serum concentrations (mean ± SEM) of MF and its metabolites following single injections of 1 mg (a) or 10 mg (b) of MF in Inhα/Tag TG mice. Effects of MF (c), P4 (d) and the 22-hydroxy, N-demethyl and Di-demethyl MF metabolites treatments (e) on KK-1 cell proliferation. Light microscopy images of cells after 5 μM or 17.5 μM MF treatment (f). Immunolocalization of HMGB1 protein after 5 μM or 17.5 μM MF treatment (g). The proliferation level of the treated groups is presented as the percentage of control proliferation, considered as 100%. Asterisks indicate significant differences between the control and treated groups (*, $P < .05$; **, $P < .01$; ***, $P < .001$; ****, $P < .0001$) (One-way ANOVA with the post-hoc Bonferroni's test). Scale bar, 20 μm. Di-demethyl MF, (11β,17β)-11-(4-Aminophenyl)-17-hydroxy-17-(1-propyn-1-yl)-estra-4,9-dien-3-one; 22-hydroxy MF, (11β,17β)-11-[4-(Dimethylamino)phenyl]-17-hydroxy-17-(3-hydroxy-1-propyn-1-yl)-estra-4,9-dien-3-one; Inhα/Tag mice; transgenic mice expressing the SV40 Taq oncogene under the inhibin α promoter; MF, mifepristone; N-demethyl MF, (11β,17β)-17-Hydroxy-11-[4-(methylamino)phenyl]-17-(1-propyn-1-yl)-estra-4,9-dien-3-one; P4, progesterone.
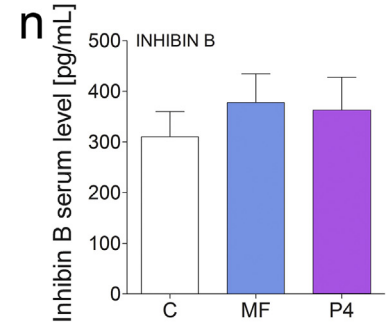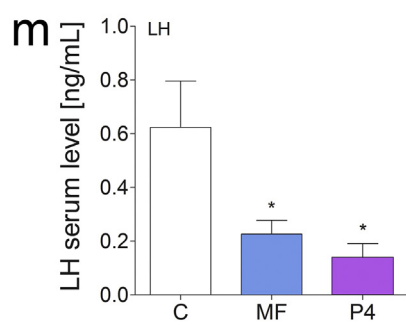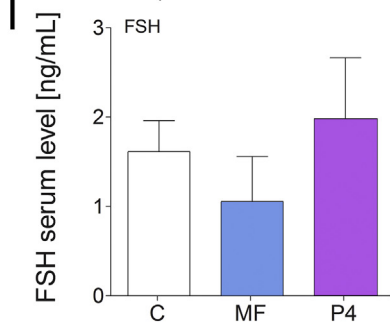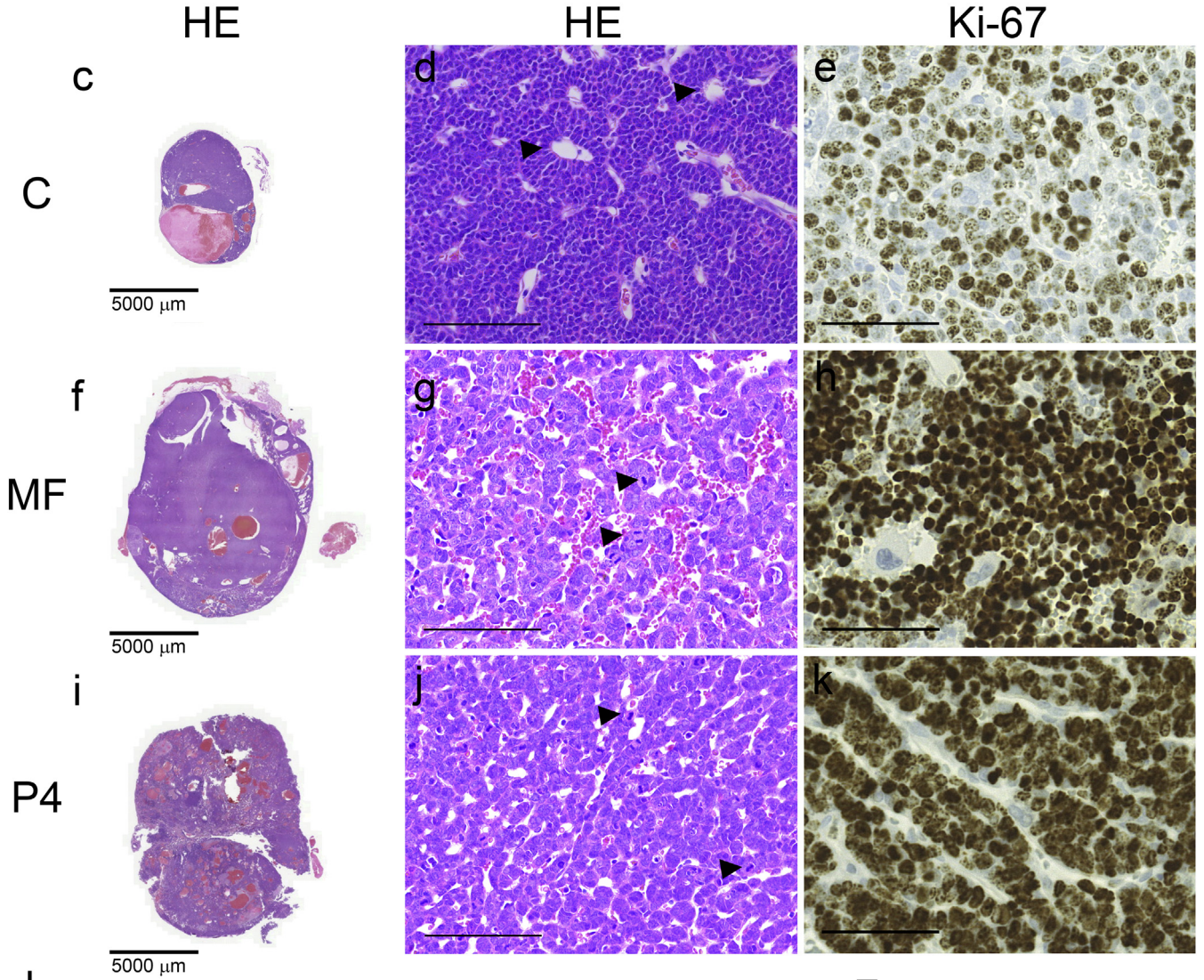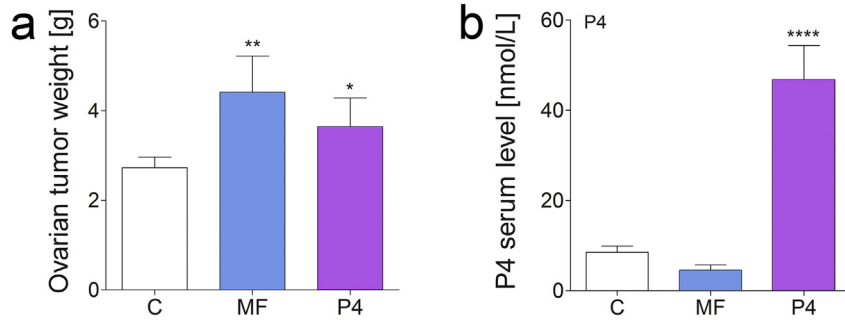
### 3.3. MF and P4 promote ovarian cancer growth in vivo

To investigate MF effects on tumor growth *in vivo* in Inhα/Tag TG mice, we chose the 10-mg/kg MF dose, which corresponded to the dose used in human clinical trials. Another group of mice was treated with 1 mg/kg P4. There were significant increases in the ovarian tumor weights after both treatments (Fig. 2a, c, f, i). Histopathological examinations revealed aggressive tumor progression (Fig. 2d). Non-treated tumors showed moderate cellular atypia, multinuclear and abnormal cells, Call-Exner bodies (arrows; Fig. 2d), and cysts surrounded by connective tissue with hyperplastic cells (Fig. 2d). The normal follicular structure remained only partially in the peripheries of non-treated tumors. The MF and P4 treatments increased cellular atypia and the number of mitotic figures to >10 per 10 high-power fields (arrows, Fig. 2g, j).

The treated tumors showed a complete lack of normal ovarian structures and the presence of an increased number of small blood vessels in the tumor mass. Tumor progression after MF or P4 treatment was confirmed by Ki-67 staining. The MF and P4 treatments increased the frequency of Ki67-positive cells to 80–90% *vs.* 60% in the non-treated group (Fig. 2e, h, k). We also observed metastases to the lungs after MF treatment in 20% of cases (2-fold increase). We assessed the hormonal profiles after the treatments. The serum levels of P4 were increased after P4 treatment (Fig. 2b). The serum FSH and inhibin B levels were unaltered in all treatment groups (Fig. 2l, n), whereas serum LH levels were reduced after the MF and P4 treatments compared to the non-treated controls (Fig. 2m).

### 3.4. MF and P4 stimulate tumor proliferation and invasiveness through PGRMC1

We screened the KK-1 cells and Inhα/Tag GCTs at the mRNA and protein levels for all types of PR (Supplementary Table S1). In the tumors, *Pgr* mRNA expression was basally very low and significantly increased only after P4 treatment (Fig. 3a). All membrane PRs (*Paqr7, Paqr8, Paqr5, Pgrmc1, Pgrmc2* and *Serbp1* (PGRMC1 cofactor)) showed clear expression that was unaffected by the MF and P4 treatments (Fig. 3b, c). *Pgrmc1* mRNA expression was highest in all groups of tumors (Fig. 3b). Immunohistochemical analysis revealed only weak local nuclear expression of PGR (Fig. 3d, f, h) but abundant cytoplasmic, perinuclear and nuclear localization of PGRMC1 in the MF- and P4-treated tumors (Fig. 3g, i). Non-treated groups of tumors also showed strong PGRMC1 staining mainly in the cytoplasm (Fig. 3e).

KK-1 cells expressed all types of PRs except for PGR at the protein level (Supplementary Table S2). To determine whether PGRMC1 mediated MF or P4 actions, we treated KK-1 cells with the PGRMC1 inhibitor AG-205. PGRMC1 blockage inhibited both MF- and P4-induced KK-1 cell proliferation (Fig. 3j). Moreover, both MF and P4 with the PGRMC1 inhibitor co-treatment decreased KK-1 cell proliferation compared to the control group (Fig. 3j). Treatment with PGRMC1 inhibitor also significantly decreased KK-1 cell migration and abolished MF- and P4-induced KK-1 cell invasion (Fig. 3k).

### 3.5. MF and P4 activate the TGFβ1 superfamily signaling pathway

As the TGFβ1 superfamily members may act as potential stimuli of cancer progression [27,28], we studied their roles in the context of this study. Both the MF and P4 treatments increased serum TGFβ1 levels in Inhα/Tag TG mice compared with non-treated mice (Fig. 4a). Both

the MF and P4 treatments significantly up-regulated *Tgfb1, TgfbrI, TgfbrII* and *Smad3* expression in the TG mouse tumors (Fig. 4b). TGFβRII was undetectable in the non-treated tumor group at both the mRNA and protein levels (Fig. 4b, c), but its protein expression was induced by the MF and P4 treatments (Fig. 4c–e). In line with the elevated serum TGFβ1 levels, the MF and P4 treatments increased TGFβ1 production by KK-1 cells, while PGRMC1 inhibition blocked this effect (Fig. 4h). Both the MF and P4 treatments also significantly up-regulated *Tgfb1* and *TgfbrII* in KK-1 cells (Fig. 4f, g). The blockage of PGRMC1 abolished the MF- and P4-dependent up-regulation of *Tgfb1* and *TgfbrII* in KK-1 cells (Fig. 4f, g).

The MF and P4 treatments, with or without recombinant TGFβ1, significantly up-regulated the proliferation of KK-1 cells in all treatment groups and showed an additive effect to MF (Supplementary Fig. S1a). Additionally, TGFβ1 significantly increased the effects of MF. MF, P4 and TGFβ1 increased KK-1 cell proliferation compared to the control, and these effects were abolished by the TGFβ1RI/RII inhibitor GW788388 (i TGFβ) (Supplementary Fig. S1b). To exclude the eventual synergistic/additive role of the Simian Virus 40 T antigen (SV40 Tag) oncogene to MF or P4 in tumor promotion, we assessed SV40 Tag expression before and after the treatments in Inhα/Tag TG mice and KK-1 cells (Supplementary Fig. S2–3). The mRNA level of *SV40 Tag* did not change after the MF or P4 treatment in tumors (Supplementary Fig. S2f). The MF, P4 or PGRMC1 inhibitor AG-205 treatments also did not affect the *SV40 Tag* expression level in KK-1 cells (Supplementary Fig. S3). Immunohistochemistry analysis showed abundant expression of the SV40 Tag protein only at the early (2–4 months) developmental stages of the tumors (Supplementary Fig. S2a, b). In the advanced stages with discernible tumors (6.5 months), the non-treated tumors showed weak protein expression, and SV40 Tag remained unchanged after both the MF and P4 treatments (Supplementary Fig. S2c–e).

### 3.6. MF and P4 stimulate high-grade (HG) human ovarian epithelial cancer (hOEC) cell proliferation through PGRMC1, independently of their glucocorticoid receptors (GRs)

To confirm the human relevance of our findings, we used patient-derived explants and primary cell cultures of HG-hOEC. As in mice, MF (up to 5 μM) (Fig. 5a) and P4 (0.003, 0.03, and 0.3 μM) (Fig. 5b), at clinically relevant doses, significantly stimulated the proliferation of the HG-hOEC cells. Higher doses of MF (from 10 to 25 μM) significantly inhibited HG-hOEC cell proliferation (Fig. 5a). Next, we analyzed the expression levels of PRs at the mRNA and protein levels in LG- and HG-hOEC cells (Supplementary Table S2, S3 and Fig. 6c–f). Abundant (positive) PGR expression was found in LG-hOEC cells (Fig. 5c, Supplementary Table S2, S3), whereas PGR expression was absent in HG-hOEC cells (Fig. 5d, Supplementary Table S2, S3).

In HG-hOEC, PGRMC1 was abundantly expressed throughout the cell, including the perinuclear region. In LG-hOEC, PGRMC1 expression was mainly confined to the cytoplasm (Fig. 5e, f and Supplementary Table S2, S3). The MF and P4 treatments significantly up-regulated *PGRMC1* in the HG-hOEC explants (Supplementary Fig. S4). The PGRMC1 inhibitor AG-205 blocked the MF- and P4-induced proliferation and invasion of HG-hOEC cells (Fig. 5g, h). We also evaluated the ability of MF to block P4 actions. MF did not inhibit P4 actions, and co-treatment with MF and P4 enhanced the proliferation of hOEC cells (Supplementary Fig. S5).

Next, we examined the role of PGRMC1 in the activation of the TGFβ1 signaling pathway *via* MF and P4 in HG-hOEC cells. The MF

**Fig. 2.** Treatment of transgenic mice presenting ovarian tumors and post-treatment hormonal values. Total ovarian tumor weights (mean ± SEM) of control, MF-treated and P4-treated Inhα/Tag TG mice (a). Serum concentrations (mean ± SEM) of P4 (b), FSH (l), LH (m) and inhibin B (n) of the non-treated (vehicle) (control), MF-treated and P4-treated Inhα/Tag TG mice. Histopathological analyses of the control (c, d), MF-treated (f, g) and P4-treated (i, j) Inhα/Tag TG mice. Immunohistochemical analyses of the Ki-67 staining of the control (e), MF-treated (h) and P4-treated (k) Inhα/Tag TG mice. Black arrows indicate Call-Exner bodies (d) or mitotic figures (g, j). Asterisks indicate significant differences between non-treated and treated groups (*, P < .05; **, P < .01; ****, P < .0001) (One-way ANOVA with the post-hoc Bonferroni's test). Original magnification, 40×; scale bar, 50 μm. C, control; Inhα/Tag mice; transgenic mice expressing the SV40 Taq oncogene under the inhibin α promoter; MF, mifepristone; P4, progesterone.
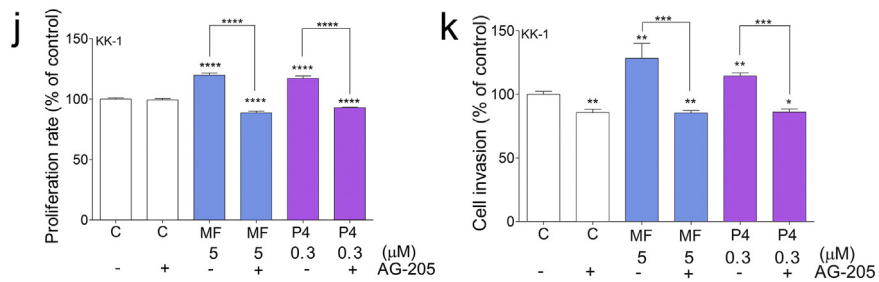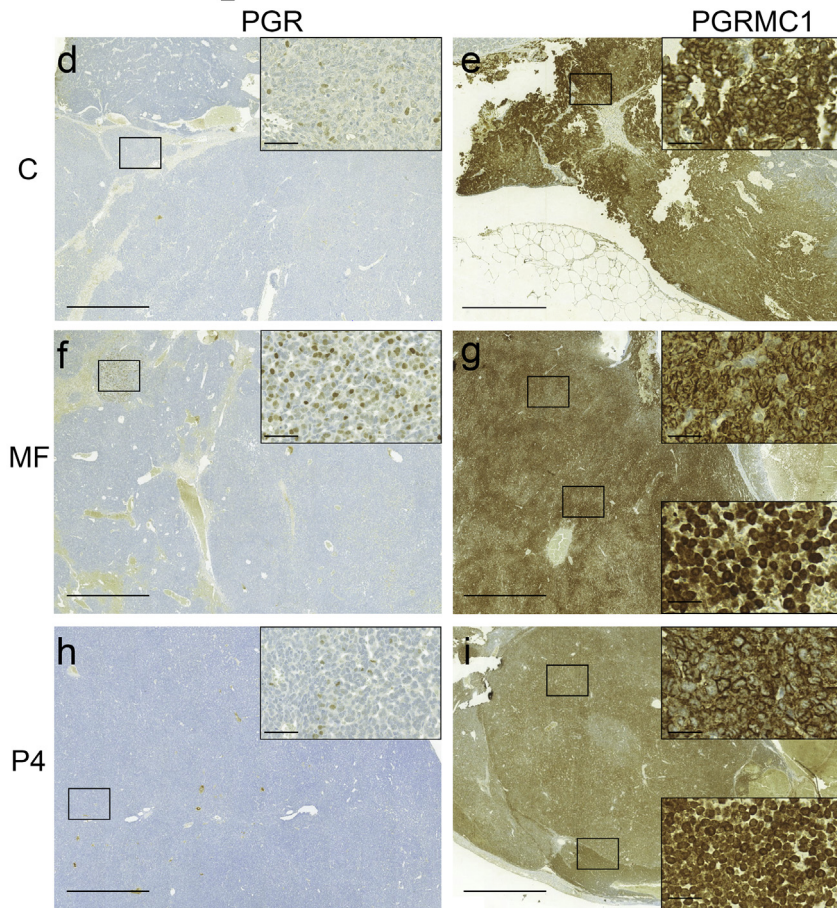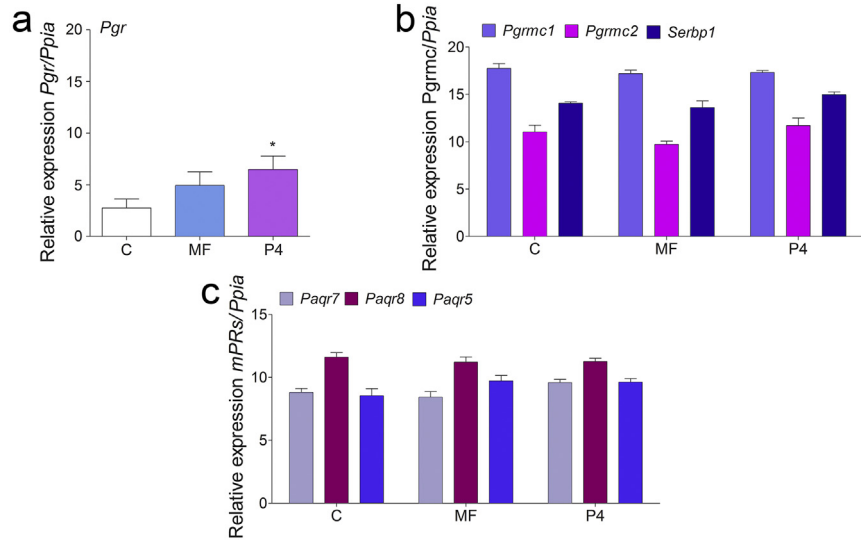
treatment of HG-hOEC tumor explants significantly increased TGFβ1 secretion, which could be blocked by PGRMC1 inhibition (Fig. 5i). The MF and P4 treatments up-regulated *TGFB1* in the HG-hOEC explants, and PGRMC1 inhibition with AG-205 abolished this effect (Fig. 5j). TGFβ1 treatment alone or together with MF or P4 significantly increased HG-hOEC cell proliferation, although the combination of TGFβ1 with MF or P4 did not have an additive or synergistic effect (Supplementary Fig. S6). We also examined the nuclear translocation of PGRMC1 after the MF and P4 treatments in HG-hOEC cells (Fig. 6). Immunostaining for the PGRMC1 signal in the control cells was evident mainly in the cytoplasm (Fig. 6a), whereas the MF or P4 treatments induced the translocation of PGRMC1 to the nucleus (Fig. 6b, c). PGRMC1 inhibition with AG-205 suppressed PGRMC1 nuclear translocation (Fig. 6d–f).

As MF actions can also be mediated through GR, we assessed the *GR* and GR-target genes expression levels [29–31] and subcellular immunolocalization in HG-hOEC after MF treatment (Supplementary Fig. S7–9). MF treatment did not have any effect on the *GR* mRNA expression levels compared to the control (Supplementary Fig. S7a). The expression level of GR-target genes *FKBP5, SKA2, OCT1* and *OCT2* also did not change in KK-1 cells (Supplementary Fig. S8a-d) and in HG-hOEC cells after the MF or P4 treatments (Supplementary Fig. S9a-d). Immunostaining for the GR signal was present in the non-treated cells in both the cytoplasm and nucleus (Supplementary Fig. S7b). The GR signal pattern of the cells treated with MF alone or with an HSP90 inhibitor was identical to that of the non-treated cells (Supplementary Fig. S7c, d). As a positive control, dexamethasone (DXM)-treated cells were used, and these cells showed GR nuclear staining (Fig. S7e); however, HSP90 inhibitor treatment suppressed the DXM-induced GR translocation to the nucleus (Supplementary Fig. S7f).

## 4. Discussion

The very promising *in vitro* data on the anti-cancer activity of MF treatment has prompted several clinical trials; however, these clinical trials, such as the hEOC trial, have been unsuccessful [1,2]. The discrepancy between experimental *in vitro* data and clinical *in vivo* data highlights the complexity of MF actions and the need for mechanistic studies. One of the limitations of this study was that besides high-grade human primary epithelial ovarian cancer (HG-hOEC) cells and their explants, we had to use Inhα/Tag TG mice presenting with endogenous GCT with 100% penetrance. Inha/Tag GCT mouse model was used because no relevant ovarian epithelial cancer models are available. The ovarian granulosa cell cancer model is not the most relevant model for human ovarian cancer, which usually originates from the epithelium. However, the Inha/Tag model seems to harbor the same components of MF action as human epithelial tumor cells, and therefore is a relevant model for unraveling the molecular mechanisms of the unexpected stimulatory effect of MF on tumor growth.

### 4.1. Serum MF and its metabolites do not reach cancer cell inhibition levels

In humans, the tissue availability of MF is limited by its rapid metabolism and binding to high-affinity binding protein α 1-acid glycoprotein (AAG). The serum concentration of ~2.5 μM corresponds to the AAG binding capacity of MF [25]. As only unbound drug is available for diffusion into target tissues to exert its pharmacological effects, the concentration of unbound MF in circulation should determine its availability at the target tissue and the efficacy of treatment [25]. Research has shown that the tissue MF concentration after the administration of 200 mg of MF is equal to or lower than the serum MF concentration [25]. In these studies, the non-protein bound fraction of MF varied from 1.9 to 3.1%, and the serum MF concentration was lower than 2.1 μM [32].

Research has also shown that the serum concentrations of MF were not affected by increasing the dose of MF [22]. At 24 h, after single oral doses of either 100, 400, 600 or 800 mg MF, the serum levels of circulating MF reached 2.5 μM in all groups [22]. The MF level in the 800-mg MF group was higher than and varied significantly from that only in the 100-mg MF group after 2 h [22]. Moreover, a similar 2.5-μM level was reached when MF was repeatedly administered in doses exceeding 100 mg/day [24]. During long-term treatment (up to 20 months), the serum concentration of MF remained similar [26].

The major active metabolite of MF, namely, *N*-demethyl MF (metapristone), has been tested for cancer treatment [32,33], but no data are available about the biological activity of other MF metabolites. Metapristone inhibits cell proliferation in a dose-dependent manner (IC$_{50}$ 53.8–83.5 μM in different cell lines), and at 40 μM, metapristone prevents cell migration after 24 h of treatment [33]. This finding is inconsistent with that of our *in vitro* experiments, which showed that treatment with metapristone significantly stimulates cell proliferation. In our experiments, the other MF metabolites did not affect cancer cell proliferation. The relative binding affinity of metapristone to PGR is 21% of that to MF, and in human serum, the binding affinity of metapristone exceeds that of MF and the remaining metabolites [23]. The tissue concentration of metapristone in patients after the ingestion of 200 mg of metapristone was lower than the serum concentration [25]. Therefore, high (pharmacological) doses of metapristone appear to not reach tissue concentrations that are high enough to achieve cancer cell inhibition, thereby making these doses clinically irrelevant.

### 4.2. MF has a biphasic effect on ovarian tumor progression

Our *in vitro* experiments demonstrated that the effect of MF on tumor cell growth is in fact biphasic and that pharmacologically relevant concentrations of MF (1–5 μM) significantly stimulate the proliferation of ovarian cancer cells. Only much higher MF concentrations have the desired *in vitro* antitumour effect. The *in vivo* treatment of 10 mg/kg/day MF (a dose corresponding to the higher dose of MF used in clinical trials) did not exceed the 5-μM serum levels in the treated mice and stimulated tumor growth *in vivo* in Inhα/Tag TG mice. Previous *in vitro* studies showed that MF at concentrations of 10 to 100 μM had antitumor activity and inhibited cancer cell growth [10–14], but at lower concentrations (1 μM), MF had no effects on HG-hOEC cells [16]. A study on SKOV3 tumor xenografts in nude mice showed the growth inhibitory effect of MF (0.5 or 1 mg/day) on ovarian cancer xenografts [10]. Taken together, these data suggest that growth inhibition with higher doses of MF cannot be achieved in tumor tissues and that MF at low levels is biologically active and may instead have a stimulatory effect. This finding provides a plausible explanation for the unexplained failures of the clinical ovarian cancer trials with MF.

### 4.3. MF actions in HG-hOEC cells are independent of GR activation

In addition to PGR, MF binds to GRs (GR isoforms α and β) with high affinity [23]. One report has indicated that MF can bind to GRβ and stimulate its nuclear translocation [34]. In contrast, another study failed to

**Fig. 3.** PR gene profiling in MF- and P4-treated transgenic Inhα/Tag mice and cell proliferation and invasion *in vitro*. qPCR analysis of *Pgr* (a), *Pgrmc1, Pgrmc2, Serbp1* (b), *Paqr7* (mPRα), *Paqr8* (mPRβ), and *Paqr5* (mPRγ) (c) expression in the non-, MF- and P4-treated tumors of Inhα/Tag TG mice. Each bar represents the mean ± SEM relative to *Ppia*. Immunohistochemical staining of PGR in the control (d), MF-treated (f) and P4-treated (h) tumors and of PGRMC1 in control (e), MF-treated (g) and P4-treated (i) tumors of Inhα/Tag TG mice. The boxes on the right show higher magnifications of the boxes outlined on the left, revealing different PR cell localizations. Original magnification, 10×; scale bar, 200 μm. Box magnification, 40×; scale bar, 50 μm. Effects of MF and P4 with or without the AG-205 inhibitor on KK-1 cell proliferation (j). Cell proliferation of the treated groups is presented as the percentage of the control (considered as 100%). Effects of MF and P4 with or without the AG-205 inhibitor on KK-1 cell invasion (k). Cell invasion of the treated groups is presented as the percentage of the control group (considered as 100%). Asterisks indicate significant differences between the control and treated groups (*, $P < .05$; **, $P < .01$; ***, $P < .001$; ****, $P < .0001$) (One-way ANOVA with the post-hoc Bonferroni's test). C, control; AG-205, PGRMC1 inhibitor; Inhα/Tag mice; transgenic mice expressing the SV40 Taq oncogene under the inhibin α promoter; MF, mifepristone; P4, progesterone.
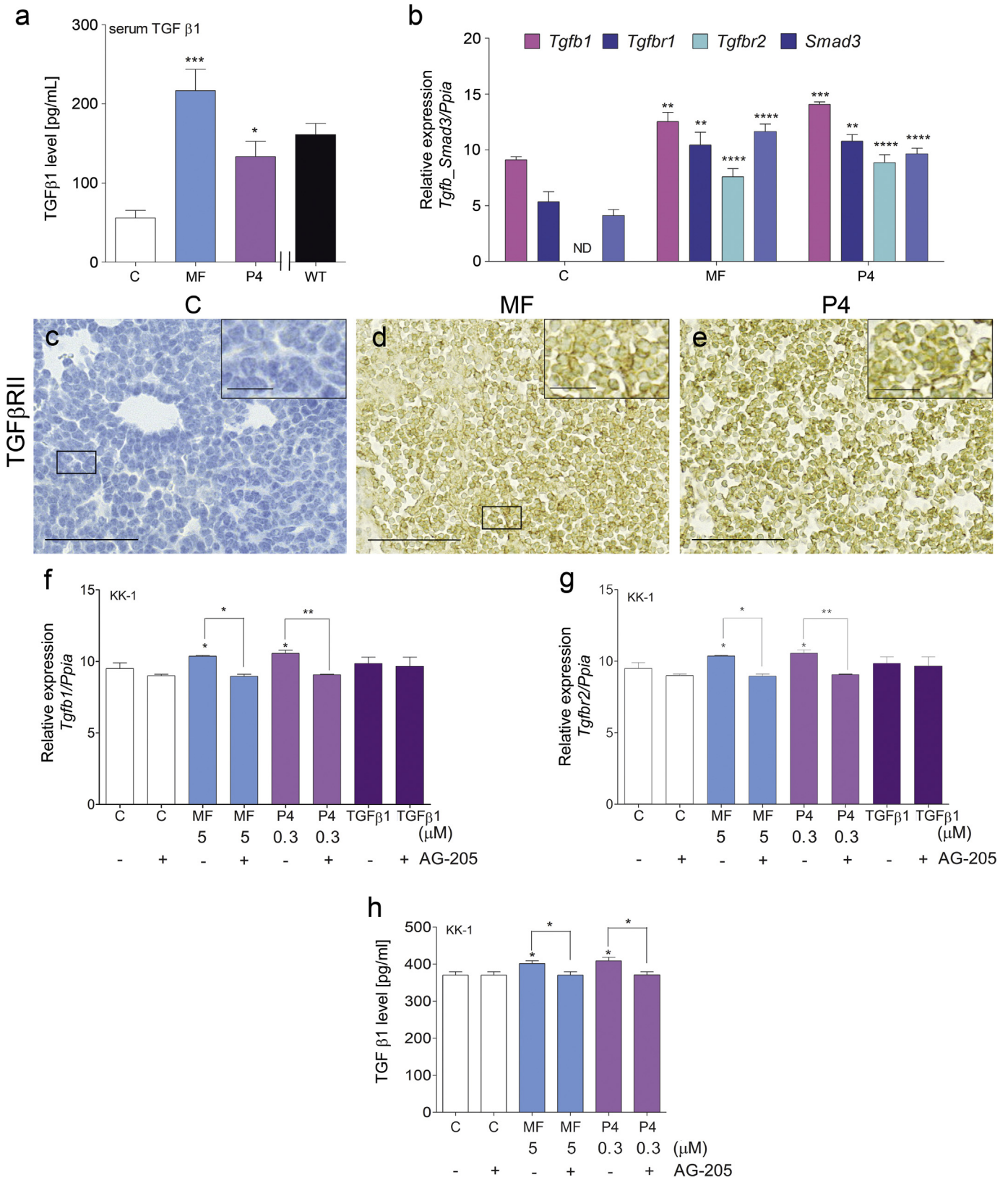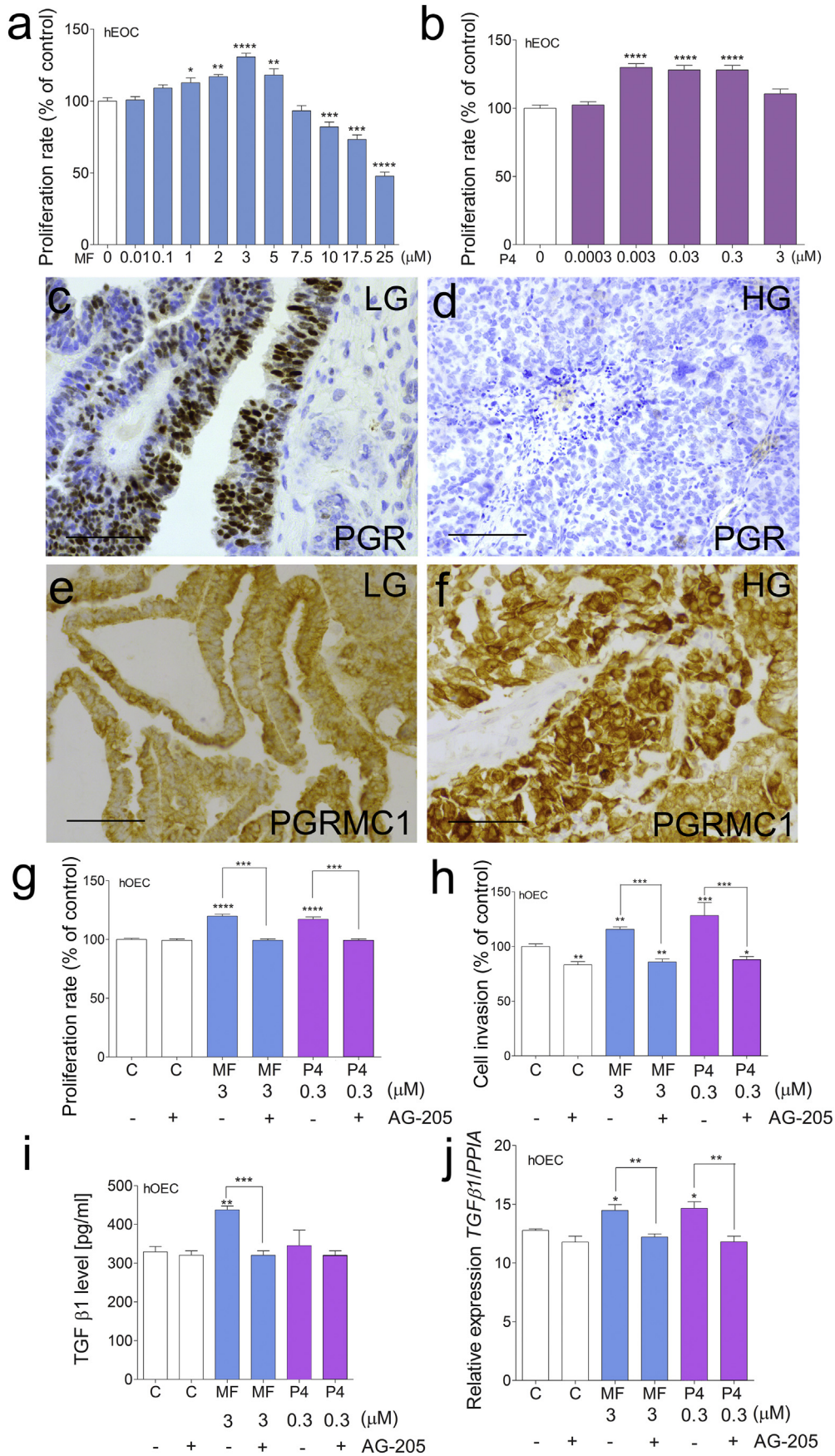
**Fig. 4.** MF and P4 treatments effect on TGFβ1 superfamily signaling pathways. TGFβ1 serum level in the control, MF-treated or P4-treated tumors of Inhα/Tag TG mice (a). qPCR analysis of the *Tgfb1, Tgfbr1, Tgfbr2* and *Smad3* expression levels in the control, MF-treated and P4-treated tumors of Inhα/Tag TG mice (b). Each bar represents the mean ± SEM relative to *Ppia*. Immunohistochemical staining of TGFβR2 in the control (c), MF-treated (d) and P4-treated (e) tumors of Inhα/Tag TG mice. The boxes on the right show higher magnifications of the boxes outlined on the left, revealing TGFβR2 cell localization. Original magnification, 40×; scale bar, 50 μm. Box magnification, 80×; scale bar, 25 μm. qPCR analysis of the *Tgfb1* and *Tgfbr2* expression levels in C, TGFβ1-treated, MF-treated and P4-treated KK-1 cells with or without the AG-205 inhibitor (f, g). TGFβ1 levels in the control, MF-treated or P4-treated KK-1 cells with or without the AG-205 inhibitor (h). Each bar represents the mean ± SEM relative to *Ppia*. Asterisks indicate significant differences between the non-treated control and treated groups (*, P < .05; **, P < .01; ***, P < .001; ****, P < .0001) (One-way ANOVA with the post-hoc Bonferroni's test). AG-205, PGMC1 inhibitor; Inhα/Tag mice; transgenic mice expressing the SV40 Taq oncogene under the inhibin α promoter; C, control; MF, mifepristone; ND, non-detectable; P4, progesterone.
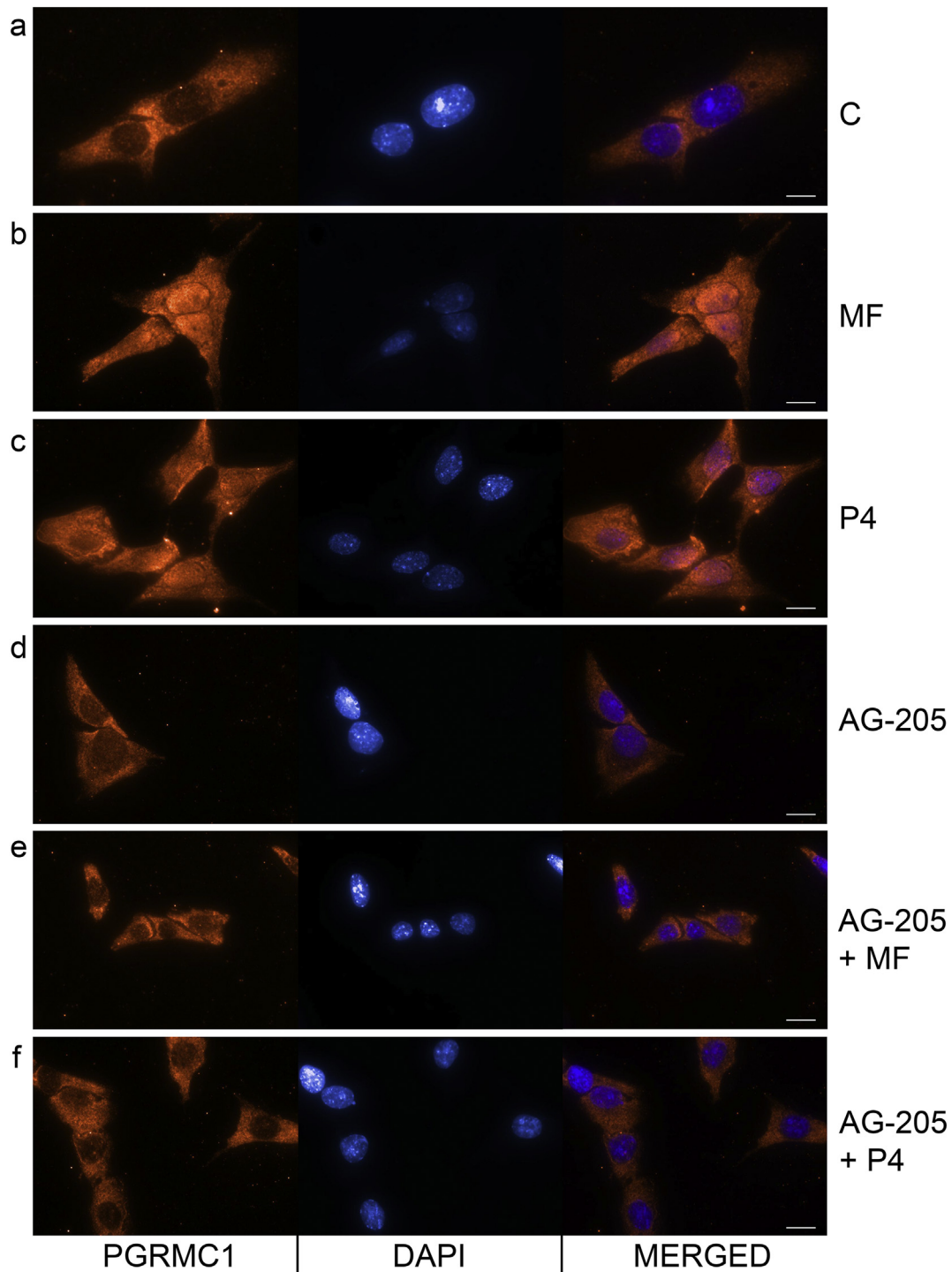
**Fig. 6.** MF and P4 treatments effect on the nuclear translocation of PGRMC1 in HG-hOEC cells. Immunocytochemical localization of PGRMC1 without C (a) or with MF (b), P4 (c), AG-205 (d), AG-205 + MF (e) and AG-205 + P4 (f) in HG-hOEC cells. Scale bar, 10 μm. AG-205, PGRMC1 inhibitor; C, control; MF, mifepristone; P4, progesterone.

show any connection between MF actions and the nuclear translocation of GRβ and activation of gene transcription [35]. Our results did not show an association between MF treatment and GR nuclear translocation and stimulation of GR-related genes expression in HG-hOEC cells, indicating that MF actions in cancer cells are not dependent on GR activation and can be mediated through other receptors, such as mPRs.

**Fig. 5.** High-grade hOEC cell proliferation after MF, P4, PGRMC1 inhibitor and TGFβ1 treatment. Effects of MF (a) or P4 (b) treatment on the proliferation HG-hOEC cells. Cell proliferation of the treated groups is presented as the percentage of the control (considered as 100%). Immunohistochemical staining of PGR in LG-hOEC (c) and HG-hOEC (d) and PGRMC1 in LG-hOEC (e) and HG-hOEC (f). Effects of MF and P4 treatments with or without the AG-205 inhibitor on HG-hOEC cell proliferation (g). Cell proliferation of the treated groups is presented as the percentage of the control (considered as 100%). Effects of MF and P4 treatments with or without the AG-205 inhibitor on HG-hOEC cell invasion (h). Cell invasion of the treated groups is presented as the percentage of the control (considered as 100%). TGFβ1 levels in C, MF-treated and P4-treated hOEC explants with or without AG-205 inhibitor (i). qPCR analysis of *TGFB1* expression levels in the control, MF-treated or P4-treated hOEC explants with or without the AG-205 inhibitor (j). Each bar represents the mean ± SEM relative to *PPIA*. Asterisks indicate significant differences between non-treated control and treated groups (*, $P < .05$; **, $P < .01$; ***, $P < .001$; ****, $P < .0001$) (One-way ANOVA with the post-hoc Bonferroni's test). Original magnification, 40×; scale bar, 50 μm. AG-205, PGRMC1 inhibitor; C, control; HG, high-grade; hOEC, human ovarian epithelial cancer; LG, low-grade; MF, mifepristone; P4, progesterone.

### 4.4. Deciphering the tumor promotion effect – a lack of PGR in ovarian cancer, but high PGRMC1

We found only marginal/traceable expression levels of PGR, low expression levels of mPRα, mPRβ, mPRγ and PGRMC2, and high expression levels of PGRMC1 in the ovarian tumors, suggesting a significant role of the latter in ovarian cancer. Abundant PGRMC1 expression has been detected in human ovarian cancers, and in advanced stages, the *PGRMC1* mRNA level increases, whereas the *PGR* mRNA level decreases [36]. These observations are consistent with our results, which showed PGR expression only in LG-hOEC and the overexpression of PGRMC1 in HG-hOEC. Recent studies have demonstrated that PGRMC1 also promotes cancer cell invasion [37]. The results of our *in vitro* studies show that PGRMC1 is required for MF and P4 to increase the invasiveness of ovarian tumor cells. We also show that PGRMC1 inhibition attenuates the abilities of MF and P4 to increase the proliferation of cancer cells. In our experiments, PGRMC1 expression in LG-hOEC was localized mainly to the cytoplasm, whereas PGRMC1 expression in HG-hOEC was present throughout the cell, including the perinuclear region. After the MF and P4 treatments, the expression of PGRMC1 in GCTs was localized to the cytoplasm and nucleus, whereas the expression of PGRMC1 in the control non-treated group was mainly cytoplasmic and perinuclear. We observed also that MF and P4 could induce PGRMC1 translocation into the nucleus in HG-hOEC cells. Altogether, MF and P4 seem to mediate their actions in these cells through PGRMC1. Thus, the differential PR status of tumors may also explain the contradictory effects of MF treatment on cancer cell survival, especially when considering that MF causes cancer progression even in PGR-positive cancers [3]. Furthermore, similar to MF therapy, clinical trials on ovarian cancer therapy with P4 have failed [38–40]. Our results therefore suggest that MF acts as a selective P4 agonist through PGRMC1 activation.

### 4.5. Unraveling the mechanism of tumor progression - involvement of TGFβ1/TGFβRII signaling through PGMRC1

The signaling pathways of the TGFβ1 superfamily are essential for processes such as cell proliferation, differentiation, apoptosis, migration and invasion [41]. In cancers, TGFβ1 may have dual roles, suppressing tumorigenesis while also acting as a promoter of tumorigenesis, depending on the cellular context and cancer stage [41]. Our analysis revealed that the MF and P4 treatments activated the TGFβ1 superfamily signaling pathways *in vitro* and *in vivo*. TGFβRII expression was undetectable in the Inhα/Tag TG mouse tumors, possibly indicating impaired anti-cancer actions of TGFβ1. The MF and P4 treatments induced TGFβRII expression and the elevation of serum TGFβ1 levels, which correlated with disease progression (*i.e.*, increased tumor growth, Ki-67 staining and metastasis in the MF-treated group) in Inhα/Tag TG mice. Microarray analysis revealed down-regulated *TGFBRII* in ovarian cancers [42], and Northern blot analysis showed reductions in *TGFBRI* and *TGFBRII* in recurrent ovarian tumors [43]. Thus, the absence of TGFβRII could be the missing link underlying cancer cell resistance to tumor-suppressive TGFβ actions. On the other hand, receptor activation in the later stages of cancer could shift TGFβ1 from its tumor-suppressive role to its tumorigenic role.

We also showed that both the MF and P4 treatments up-regulated *TGFB1* expression levels in KK-1 and HG-hOEC cells. The expression of TGFβ 1, 2 and 3 has been reported in human ovarian tumors [44,45]. In the advanced stages of ovarian cancer, TGFβs enhance cancer cell proliferation [28]. Furthermore, the increased expression of TGFβs in ovarian cancers has been associated with metastasis and a poor prognosis [27]. A significant correlation has been found between TGFβ1 serum levels and disease stage. An elevated serum level of TGFβ1 has also been associated with metastasis [46]. Our experiments showed that both the MF or P4 treatments increased TGFβ1 release by KK-1 cells and HG-hOEC explants, whereas PGRMC1 inhibition significantly

reduced the treatment effects on TGFβ1 production. PGRMC1 was also involved in the MF and P4 effects on *TGFB1* and *TGFB1RII* in KK-1 cells and HG-hOEC explants. Taken together, our results indicate that both MF and P4 switch the TGFβ1 function towards a tumor-promoting mode through PGRMC1. We tried several times to get the tissue blocks from the MF clinical trials, but without any success. This could have compellingly established the activation of this pathway as the underlying cause for the observed lack of efficacy of mifepristone in clinical trials in ovarian cancer.

An effective anti-cancer therapy drug should be able to penetrate and achieve a therapeutic concentration in the tumor tissue to induce a cytostatic effect. The tissue concentration of MF is limited, and thus, the therapeutic effect of higher doses of MF may not be achieved in cancer tissues. Based on previous clinical trial failures with ovarian cancers and on the present data, low concentrations of MF may promote the growth of ovarian cancers. Our studies indicate that MF may act as a membrane PR agonist, which explains how MF can maintain tumor progression in cells. The beneficial antitumor effect of high doses of MF cannot be achieved in human cancer tissue, and the therapeutic concentrations reach only low concentrations, with tumor-promoting effects. Therefore, MF should not be used in anti-cancer therapy due to its agonistic and tumor progression-enhancing activity. PGRMC1 inhibitors can provide an important therapeutic means for the treatment of HG-hOEC.

### Author contributions

Donata Ponikwicka-Tyszko, Marcin Chrusciel, Slawomir Wolczynski and Nafis A Rahman designed the research; Donata Ponikwicka-Tyszko, Marcin Chrusciel, Joanna Stelmaszewska, Piotr Bernaczyk, Paulina Chrusciel, Maria Sztachelska, Mika Scheinin, Mariusz Bidzinski, Jacek Szamatowicz acquired the data and performed the experiments; Donata Ponikwicka-Tyszko, Ilpo Huhtaniemi, Slawomir Wolczynski and Nafis A Rahman wrote the manuscript.

All authors read and approved the final version of the manuscript.

### Declaration of Competing Interest

The authors have no conflicts of interest.

### Appendix A. Supplementary data

Supplementary data to this article can be found online at https://doi.org/10.1016/j.ebiom.2019.08.035.

### References

[1] Rocereto TF, Saul HM, Aikins Jr JA, Paulson J. Phase II study of mifepristone (RU486) in refractory ovarian cancer. Gynecol Oncol 2000;77:429–32.

[2] Rocereto TF, Brady WE, Shahin MS, Hoffman JS, Small L, Rotmensch J, et al. A phase II evaluation of mifepristone in the treatment of recurrent or persistent epithelial ovarian, fallopian or primary peritoneal cancer: a gynecologic oncology group study. Gynecol Oncol 2010;116:332–4.

[3] Ramondetta LM, Johnson AJ, Sun CC, Atkinson N, Smith JA, Jung MS, et al. Phase 2 trial of mifepristone (RU-486) in advanced or recurrent endometrioid adenocarcinoma or low-grade endometrial stromal sarcoma. Cancer 2009;115:1867–74.

[4] Ho PC, Yu Ng EH, Tang OS. Mifepristone: contraceptive and noncontraceptive uses. Curr Opin Obstet Gynecol 2002;14:325.

[5] Perrault D, Eisenhauer EA, Pritchard KI, Panasci L, Norris B, Vandenberg T, et al. Phase II study of the progesterone antagonist mifepristone in patients with untreated

metastatic breast carcinoma: a National Cancer Institute of Canada Clinical Trials Group study. J Clin Oncol 1996;14:2709–12.

[6] Grunberg SM, Weiss MH, Russell CA, Spitz IM, Ahmadi J, Sadun A, et al. Long-term administration of mifepristone (RU486): clinical tolerance during extended treatment of meningioma. Cancer Invest 2006;24:727–33.

[7] Meyer ME, Pornon A, Ji JW, Bocquel MT, Chambon P, Gronemeyer H. Agonistic and antagonistic activities of RU486 on the functions of the human progesterone receptor. EMBO J 1990;9:3923–32.

[8] Bottino MC, Cerliani JP, Rojas JM, Giulianelli S, Soldati R, Mondillo C, et al. Classical membrane progesterone receptors in murine mammary carcinomas: agonistic effects of progestins and RU-486 mediating rapid non-genomic effects. Breast Cancer Res Treat 2011;126:621–36.

[9] Peluso JJ. Multiplicity of progesterone's actions and receptors in the mammalian ovary. Biol Reprod 2006;75:2–8.

[10] Goyeneche AA, Caron RW, Telleria CM. Mifepristone inhibits ovarian cancer cell growth in vitro and in vivo. Clin Cancer Res 2007;13:3370–9.

[11] Freeburg EM, Goyeneche AA, Seidel EE, Telleria CM. Resistance to cisplatin does not affect sensitivity of human ovarian cancer cell lines to mifepristone cytotoxicity. Cancer Cell Int 2009;9.

[12] Tieszen CR, Goyeneche AA, Brandhagen BN, Ortbahn CT, Telleria CM. Antiprogestin mifepristone inhibits the growth of cancer cells of reproductive and non-reproductive origin regardless of progesterone receptor expression. BMC Cancer 2011;11:207.

[13] Gamarra-Luques CD, Goyeneche AA, Hapon MB, Telleria CM. Mifepristone prevents repopulation of ovarian cancer cells escaping cisplatin-paclitaxel therapy. BMC Cancer 2012;12:200.

[14] Fauvet R, Dufournet Etienne C, Poncelet C, Bringuier AF, Feldmann G, Darai E. Effects of progesterone and anti-progestin (mifepristone) treatment on proliferation and apoptosis of the human ovarian cancer cell line, OVCAR-3. Oncol Rep 2006;15:743–8.

[15] Klijn JG, de Jong FH. Antiprogestins, a new form of endocrine therapy for human breast cancer. Cancer Res 1989;49:2851–6 Clin Cancer Res.

[16] Stringer-Reasor EM, Baker GM, Skor MN, Kocherginsky M, Lengyel E, Fleming GF, et al. Glucocorticoid receptor activation inhibits chemotherapy-induced cell death in high-grade serous ovarian carcinoma. Gynecol Oncol 2015;138:656–62.

[17] Fong MY, Kakar SS. Ovarian cancer mouse models: a summary of current models and their limitations. J Ovarian Res 2009;2.

[18] Kananen K, Markkula M, Rainio E, Su JG, Hsueh AJ, Huhtaniemi IT. Gonadal tumorigenesis in transgenic mice bearing the mouse inhibin alpha-subunit promoter/simian virus T-antigen fusion gene: characterization of ovarian tumors and establishment of gonadotropin-responsive granulosa cell lines. Mol Endocrinol 1995;9:616–27.

[19] Rahman NA, Huhtaniemi IT. Ovarian tumorigenesis in mice transgenic for murine inhibin alpha subunit promoter-driven simian virus 40 T-antigen: ontogeny, functional characteristics, and endocrine effects. Biol Reprod 2001;64:1122–30.

[20] Haavisto AM, Pettersson K, Bergendahl M, Perheentupa A, Roser JF, Huhtaniemi I. A supersensitive immunofluorometric assay for rat luteinizing hormone. Endocrinology 1993;132:1687–91.

[21] van Casteren JI, Schoonen WG, Kloosterboer HJ. Development of time-resolved immunofluorometric assays for rat follicle-stimulating hormone and luteinizing hormone and application on sera of cycling rats. Biol Reprod 2000;62:886–94.

[22] Heikinheimo O, et al. Metabolism and serum binding of RU 486 in women after various single dose human reproduction. Hum Reprod 1987;2:379–85.

[23] Heikinheimo O, Kontula K, Croxatto H, Spitz I, Luukkainen T, Lahteenmaki P. Plasma concentrations and receptor binding of RU 486 and its metabolites in humans. J Steroid Biochem 1987;26:279–84.

[24] Heikinheimo O. Pharmacokinetics of the antiprogesterone RU486 in women during multiple dose administration. J Steroid Biochem 1989;32:21–5.

[25] Heikinheimo O, Haukkamaa M, Lahteenmaki P. Distribution of RU 486 and its demethylated metabolites in humans. J Clin Endocrinol Metab 1989;68:270–5.

[26] Heikinheimo O, Ranta S, Grunberg S, Spitz I. Alterations in the pituitary- thyroid and pituitary-adrenal axes—consequences of long- term mifepristone treatment. Metabolism 1997;46:292–6.

[27] Nakanishi Y, Kodama J, Yoshinouchi M, Tokumo K, Kamimura S, Okuda H, et al. The expression of vascular endothelial growth factor and transforming growth factor-beta associates with angiogenesis in epithelial ovarian cancer. Int J Gynecol Pathol 1997;16:256–62.

[28] Chou JL, Chen LY, Lai HC, Chan MW. TGF-beta: friend or foe? The role of TGF-beta/SMAD signaling in epigenetic silencing of ovarian cancer and its implication in epigenetic therapy. Expert Opin Ther Targets 2010;14:1213–23.

[29] Rice L, Waters CE, Eccles J, Garside H, Sommer P, Kay P, et al. Identification and functional analysis of SKA2 interaction with the glucocorticoid receptor. J Endocrinol 2008;198:499–509.

[30] Prefontaine GG, Lemieux ME, Giffin W, Schild-Poulter C, Pope L, LaCasse E, et al. Recruitment of octamer transcription factors to DNA by glucocorticoid receptor. Mol Cell Biol 1998;18:3416–30.

[31] Vermeer H, Hendriks-Stegeman BI, van der Burg B, van Buul-Offers SC, Jansen M. Glucocorticoid-induced increase in lymphocytic FKBP51 messenger ribonucleic acid expression: a potential marker for glucocorticoid sensitivity, potency, and bioavailability. J Clin Endocrinol Metab 2003;88:277–84.

[32] Yu S, et al. Pharmacoproteomic analysis reveals that metapristone (RU486 metabolite) intervenes E-cadherin and vimentin to realize cancer metastasis chemoprevention. Sci Rep 2016;6.

[33] Wang J, Chen J, Wan L, Shao J, Lu Y, Zhu Y, et al. Synthesis, spectral characterization, and in vitro cellular activities of metapristone, a potential cancer metastatic chemopreventive agent derived from mifepristone (RU486). AAPS J 2014;16:289–98.

[34] Lewis-Tuffin LJ, Jewell CM, Bienstock RJ, Collins JB, Cidlowski JA. Human glucocorticoid receptor beta binds RU-486 and is transcriptionally active. Mol Cell Biol 2007;27:2266–82.

[35] Kino T, et al. Glucocorticoid receptor (GR) beta has intrinsic, GRalpha-independent transcriptional activity. Biochem Biophys Res Commun 2009;381:671–5.

[36] Peluso JJ, Liu X, Saunders MM, Claffey KP, Phoenix K. Regulation of ovarian cancer cell viability and sensitivity to cisplatin by progesterone receptor membrane component-1. J Clin Endocrinol Metab 2008;93:1592–9.

[37] Ahmed IS, Rohe HJ, Twist KE, Mattingly MN, Craven RJ. Progesterone receptor membrane component 1 (Pgrmc1): A Heme-1 domain protein that promotes tumorigenesis and is inhibited by a small molecule. J Pharmacol Exp Ther 2010;333:564–73.

[38] Ho SM. Estrogen, progesterone and epithelial ovarian cancer. Reprod Biol Endocrinol 2003;1:73.

[39] Belinson JL, McClure M, Badger G. Randomized trial of megestrol acetate vs. megestrol acetate/tamoxifen for the management of progressive or recurrent epithelial ovarian carcinoma. Gynecol Oncol 1987;28:151–5.

[40] Veenhof CH, van der Burg ME, Nooy M, Aalders JG, Pecorelli S, Oliveira CF, et al. Phase II study of high-dose megestrol acetate in patients with advanced ovarian carcinoma. Eur J Cancer 1994;30A:697–8.

[41] Bierie B, Moses HL. TGF-beta and cancer. Cytokine Growth Factor Rev 2006;17:29–40.

[42] Sunde JS, et al. Expression profiling identifies altered expression of genes that contribute to the inhibition of transforming growth factor-beta signaling in ovarian cancer. Cancer Res 2006;66:8404–12.

[43] Bristow RE, Baldwin RL, Yamada SD, Korc M, Karlan BY. Altered expression of transforming growth factor-beta ligands and receptors in primary and recurrent ovarian carcinoma. Cancer 1999;85:658–68.

[44] Do TV, Kubba LA, Du H, Sturgis CD, Woodruff TK. Transforming growth factor-beta1, transforming growth factor-beta2, and transforming growth factor-beta3 enhance ovarian cancer metastatic potential by inducing a Smad3-dependent epithelial-to-mesenchymal transition. Mol Cancer Res 2008;6:695–705.

[45] Bartlett JM, Langdon SP, Scott WN, Love SB, Miller EP, Katsaros D, et al. Transforming growth factor-beta isoform expression in human ovarian tumours. Eur J Cancer 1997;33:2397–403.

[46] Tas F, Karabulut S, Serilmez M, Ciftci R, Duranyildiz D. Clinical significance of serum transforming growth factor-beta 1 (TGF-β1) levels in patients with epithelial ovarian cancer. Tumour Biol 2014;35:3611–6.